Ecological Indicators 178 (2025) 114066

Contents lists available at ScienceDirect

Ecological Indicators

journal homepage: www.elsevier.com/locate/ecolind

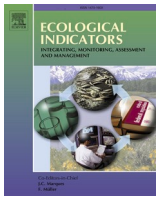

Original Articles

Shifting frontiers of nitrogen pollution: A multi-scale assessment of long-term anthropogenic nitrogen inputs across the Yellow River basin

Jincheng Li [a,b], Zhonghua Li [c,d,*], Qiang Wang [c,d], Yan Chen [c,d,*], Xinyue Zhang [e,f], Taher Kahil [b], Dor Fridman [b]

[a] Key Laboratory of Ecology and Environment in Minority Areas, Minzu University of China, National Ethnic Affairs Commission, Beijing, China
[b] Water Security Research Group, Biodiversity and Natural Resources Program, International Institute for Applied Systems Analysis (IIASA), Schlossplatz 1, A-2361 Laxenburg, Austria
[c] Chinese Academy of Environmental Planning, Beijing 100041, China
[d] Yellow River Ecology and Environment Protection Center, Chinese Academy of Environmental Planning, Beijing 100041, China
[e] State Key Laboratory of Simulation and Regulation of Water Cycle in River Basin, Beijing, China
[f] China Institute of Water Resources and Hydropower Research (IWHR), Beijing, China

ARTICLE INFO

Keywords:
Net Anthropogenic Nitrogen Input
Yellow River Basin
Spatiotemporal Analysis
Environmental Kuznets Curve
Nitrogen Management Zoning

ABSTRACT

Understanding the spatial–temporal dynamics and socioeconomic drivers of anthropogenic nitrogen inputs is essential for effective nutrient management in large river basins. This study presents a comprehensive assessment of net anthropogenic nitrogen input (NANI) in the Yellow River Basin from 1980 to 2020. It integrates multi-source statistical data from national, provincial, and prefecture-level yearbooks within a hierarchical spatial framework that includes the full basin as well as secondary and tertiary sub-basins. The results show that the NANI increases by 108.9% over the study period, accompanied by a clear shift in spatial patterns. Nitrogen inputs grow most rapidly in historically low-input upstream areas, forming a "reverse growth" trend. Centroid trajectory analysis reveals a northwestward shift in nitrogen input hotspots, primarily driven by land use change and agricultural expansion. A segmented environmental kuznets curve (EKC) model identifies a turning point in per capita GDP (41,000–46,000 CNY), beyond which nitrogen inputs begin to decline. This turning point has already been reached in the midstream and downstream regions, while the upstream region continues to experience growth. Despite recent signs of decline in basin-wide nitrogen inputs since 2016, the persistence of ecological risks and the emergence of new pollution frontiers, especially in sensitive upstream zones, highlight the need for continued attention. These spatial and temporal analyses jointly reveal the "shifting frontiers" of nitrogen pollution, defined as inflection zones where input dynamics begin to transition—spatially, temporally, or economically. This study provides methodological innovation and practical insights for improving nitrogen governance in the Yellow River Basin.

1. Introduction

Nitrogen (N) cycling is a fundamental biogeochemical process within Earth's biosphere, and it has been significantly accelerated by human activities at an unprecedented rate (Lai et al., 2022; Socolow, 2016; Zhang et al., 2020). The large-scale anthropogenic production and utilization of nitrogen have notably enhanced industrial and agricultural productivity, driving substantial socioeconomic development (Huang et al., 2021; Liu et al., 2018). However, this comes at an environmental cost, leading to adverse effects such as water eutrophication, soil acidification, and air pollution (Cai et al., 2011; Wu et al., 2022a). Currently, more than half of the world's most severe environmental issues are attributed to excessive anthropogenic N inputs, with N imbalance-induced pollution becoming increasingly critical in many countries and regions (Rockstroem et al., 2023; Sun et al., 2021). River basins, acting as critical interfaces between natural ecosystems and human societies, are particularly susceptible to nitrogen overload. Excessive nitrogen accumulation that surpasses basin carrying capacities can significantly degrade water quality, posing substantial risks to public health and economic sustainability (Chellaiah et al., 2024; Chen et al., 2024a). Therefore, the long-term and effective control of anthropogenic nitrogen inputs is essential for protecting and improving basin water

* Corresponding authors..
E-mail addresses: lizh@caep.org.cn (Z. Li), chenyan@caep.org.cn (Y. Chen).

https://doi.org/10.1016/j.ecolind.2025.114066
Received 22 July 2025; Received in revised form 14 August 2025; Accepted 14 August 2025
Available online 21 August 2025

quality. Accurate quantification of nitrogen inputs and a thorough understanding of their spatial distribution patterns have emerged as critical scientific and management priorities to achieve sustainable water-environment development.

Accurately assessing the long-term dynamics of nitrogen inputs within river basins is fundamental to effective pollution control and water quality improvement. The net anthropogenic nitrogen input (NANI) model provides a systematic framework for quantifying human-induced nitrogen inputs based on a mass balance approach and socio-economic statistical data (Howarth et al., 1996; Pei et al., 2022). This approach is particularly valuable in data-scarce regions, offering a practical and reliable means to evaluate nitrogen inputs across diverse spatial and temporal scales (Han et al., 2020). Owing to its simplicity, data accessibility, and robust performance, the NANI model has been widely applied in various national and regional contexts (Li et al., 2024a; Wang et al., 2024b). Importantly, a significant proportion of anthropogenic N is retained in soils and groundwater, where it can be gradually released over years or even decades, posing long-term risks to aquatic environments (Chen et al., 2018; Liu et al., 2023). For instance, studies in the Mississippi River Basin have shown that legacy nitrogen may account for up to 55 % of current riverine N export, with effects lasting for decades (Van Meter et al., 2017). In China, although the use of synthetic N fertilizers in croplands has declined in recent years, other sources, such as atmospheric deposition and livestock waste, have emerged as dominant contributors (Chen et al., 2023; Wang et al., 2024a). These trends underscore the need for long-term, high-resolution assessments of historical nitrogen inputs to inform basin-specific pollution control strategies. A key factor influencing the accuracy of NANI model outputs is the parameterization of nitrogen sources. In large-scale studies, substantial heterogeneity in natural and socioeconomic conditions demands localized parameter settings. Uniform assumptions across diverse regions may introduce considerable bias. For example, the N fixation capacity of soybeans can vary more than fivefold depending on local conditions (Pei et al., 2022). Therefore, applying region-specific parameters is critical to ensure the precision of NANI estimates and to support the development of targeted and scientifically grounded nitrogen management policies.

There is an urgent need for targeted research on N input management strategies for the Yellow River Basin (YRB), a region of critical ecological and strategic importance to China. Over the past four decades, China's GDP has increased by over 220-fold, and the urbanization rate has risen from 19.39 % to 63.89 %, driving profound changes in N input patterns (Chen et al., 2021; Fu et al., 2024; Huo et al., 2022). The Yellow River, often referred to as the "Mother River of China", faces a unique combination of fragile ecosystems and severe water scarcity, which amplifies its vulnerability to nitrogen pollution (Lai et al., 2024; Zhang and Oki, 2024). In 2019, the Chinese government launched the national strategy for "Ecological Protection and High-Quality Development of the Yellow River Basin," aiming to coordinate ecological restoration with sustainable socioeconomic growth (Chen et al., 2024b; Tian and Mu, 2024). However, the basin's regions exhibit substantial heterogeneity in development stages and environmental management capacities, which poses a significant challenge to implementing effective nitrogen control strategies. To address spatial heterogeneity, China's 13th Five-Year Plan (2016–2020) introduced a "Three-Tier Zoning Water Environment Management System" at the basin, sub-basin, and control unit levels (Wang et al., 2019; Wang et al., 2020; Wu et al., 2022b). At the basin level, overarching priorities and pollution control directions are defined. At the control zone level, the focus shifts to delineating ecological functions and protection needs. At the control unit level, specific pollution reduction targets, action plans, and infrastructure projects are implemented. Despite this framework, most existing studies remain focused at the provincial or municipal scale, and comprehensive, long-term assessments of N inputs at the control unit scale are still lacking (Han et al., 2014; Pei et al., 2022; Wang et al., 2024b; Wu et al., 2022b). The limited exploration of basin-wide nitrogen control strategies hinders the effectiveness of current policies. Therefore, a fine-resolution evaluation of anthropogenic nitrogen inputs at the control unit (tertiary sub-basin) scale is urgently needed. Such an approach will provide the scientific basis for regionally tailored N management policies, supporting the overarching goals of ecological protection and sustainable development in the Yellow River Basin.

Based on survey and statistical yearbook data from prefecture-level cities across the YRB from 1980 to 2020, this study develops a localized NANI model to quantify nitrogen inputs at the tertiary sub-basin (control unit) scale over the past four decades. To capture the spatio-temporal variation of nitrogen inputs and their source components, we integrate centroid trajectory analysis to track spatial migration patterns, and time-series K-means clustering to classify sub-basins into distinct developmental trajectories based on nitrogen input intensity and growth rate. Together, these approaches enable the identification of the "shifting frontiers" of nitrogen pollution—conceptualized in this study as the evolving spatial, temporal, and socioeconomic boundaries where marked transitions in nitrogen dynamics are observed. These frontiers encompass potential temporal inflection points, spatial redistribution zones, and economic thresholds where nitrogen input trajectories begin to diverge. This integrated framework facilitates a multi-scale understanding of nitrogen input patterns, and supports the delineation of targeted management zoning. The main contributions of this study: (1) it provides the first long-term, high-resolution assessment of NANI at the tertiary sub-basin scale across the Yellow River Basin; (2) it introduces a "shifting frontiers" lens to capture spatial, temporal, and socioeconomic transitions in nitrogen dynamics; (3) it develops a cluster-based zoning framework to guide differentiated and actionable nitrogen management. By identifying spatiotemporal differences in nitrogen input trends, this study offers practical insights for optimizing control strategies and advancing the region-specific, sustainable management of the basin's water environment.

2. Methods

2.1. Study area

Originating from the Qinghai-Tibet Plateau, the Yellow River extends for 5,464 km with a basin area of 795,000 km2, ranking as the world's fifth-longest river and China's second-longest (Ma et al., 2024). It flows through nine provinces and 76 prefecture-level cities. Per capita water availability is only 587 m3, equivalent to 29 % of the national average. The basin supports approximately 12.2 % of the national population and contributes 12.7 % of the country's grain output. However, its water quality lags behind that of other key basins, such as the Yangtze and Pearl River. In 2020, water classified as I-III, IV-V, below-V accounted for 82.7 %, 4.2 % and 13.1 %, respectively. This poor water quality represents a major obstacle to the sustainable development of the basin's water environment. Consistent with China's "Three-Tier Zoning Water Environment Management System" for key river basins, this study divides the Yellow River Basin into 28 secondary sub-basins (Fig. 1) and 347 tertiary sub-basin units (Fig.S1). These sub-basin units serve as the primary spatial scale for analyzing the spatio-temporal evolution of NANI.

2.2. Data sources

This study compiled multi-source statistical data to estimate nitrogen input for the Yellow River Basin at the tertiary control unit level from 1980 to 2020. Core datasets were derived from the China Statistical Yearbook, China Rural Statistical Yearbook, China Animal Husbandry and Veterinary Yearbook, and provincial and municipal statistical yearbooks of the nine provinces traversed by the Yellow River. To address spatial consistency across decades, we standardized all sub-basin-to-prefecture mappings using 2000-based administrative boundaries, following the official dataset from the Ministry of Civil Affairs of

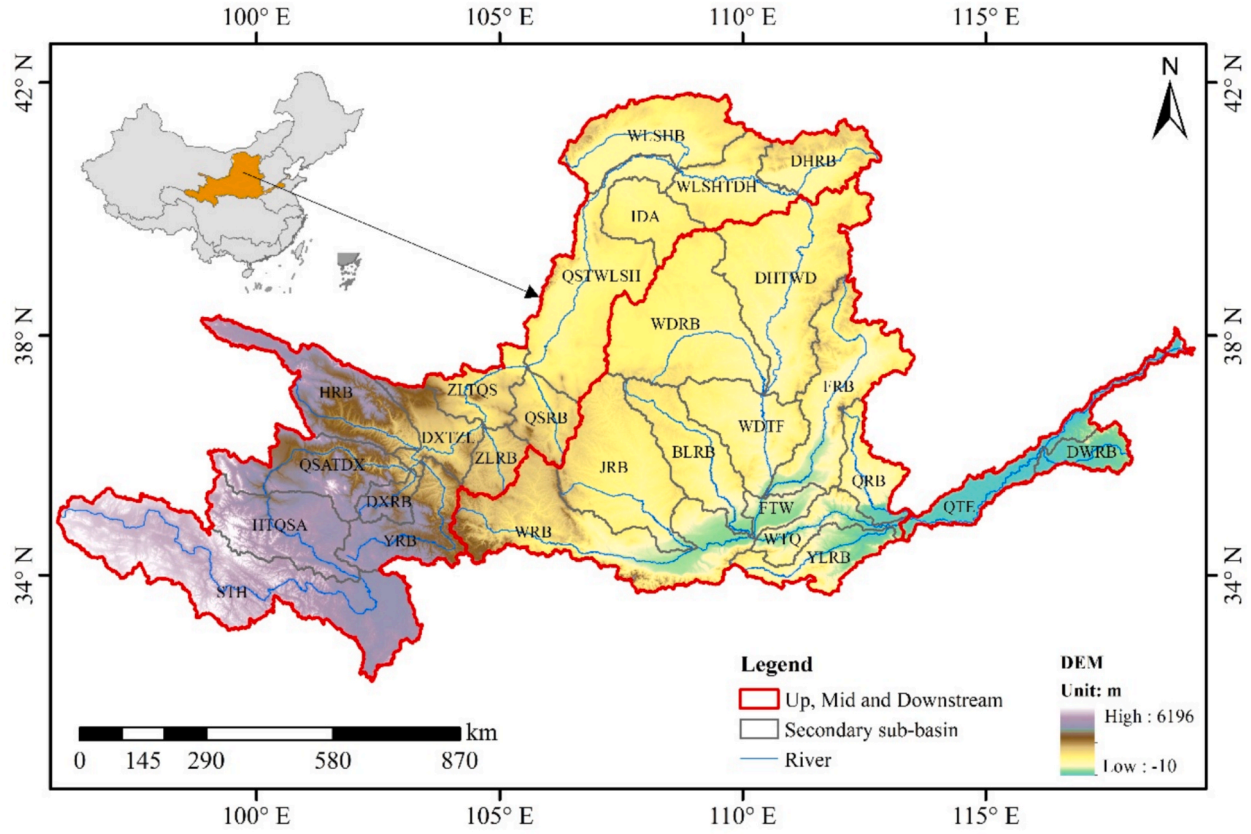

Fig. 1. Location, DEM and secondary sub-basins (abbreviations in Table S1) of the Yellow River Basin. (For interpretation of the references to colour in this figure legend, the reader is referred to the web version of this article.)

China ("National Administrative Division Information Platform": http://xzqh.mca.gov.cn/map). To ensure consistency with the latest watershed-based environmental management frameworks, which prioritize sub-basin units over administrative boundaries, this study transformed prefecture-level statistical data into hydrologically defined sub-basin units. Specifically, nitrogen input data originally reported at the prefectural level were reallocated to 347 tertiary sub-basins based on proportional downscaling using weighting factors such as urban and rural population, agricultural land area, and local GDP. These weighting variables were selected to match the spatial characteristics and dominant drivers of each nitrogen input component. The specific downscaling criteria used for each component of the NANI framework are detailed in Table S2. For early years (particularly 1980–1990, Fig. S1), where subnational data were sparse, we reconstructed inputs by applying the average intra-provincial ratios during 1990–2000, assuming these patterns remained reasonably stable backward in time. This assumption is consistent with prior NANI estimations in China (Han et al., 2014; Li et al., 2024a). To address administrative reclassifications and ensure temporal consistency, we applied moving average smoothing and exponential interpolation techniques to normalize abrupt changes and fill gaps. For example, synthetic fertilizer application and BNF rates were interpolated using multi-year averages, while feed import nitrogen was estimated by combining livestock production data with feed demand coefficients. Atmospheric nitrogen deposition was extracted from the published datasets, with spatial downscaling using gridded deposition maps and sub-basin areal weighting (Gao et al., 2020; Yu et al., 2019). Validation of the reconstructed dataset followed a three-tiered approach: (1) Summation and Consistency Checks: Sub-basin-level inputs were aggregated and compared with provincial and basin-wide totals. Deviations above ± 5 % triggered re-examination. (2) Trend and Volatility Analysis: Interannual variability was assessed to identify anomalies due to reporting changes or statistical revisions. (3) Cross-Referencing with Literature: Our NANI estimates were benchmarked against published studies on nitrogen budgets in Chinese basins (Han et al., 2014; Wang et al., 2024b), ensuring alignment with established ranges. We compared the NANI values calculated from the original and corrected datasets (Fig. S2). The results show strong consistency (R^2 = 0.9925), indicating that the correction process introduced minimal bias and that the adjusted dataset is robust for long-term spatiotemporal analysis. Overall, this data reconstruction approach balances statistical reliability and spatial resolution, enabling robust long-term trend and spatial heterogeneity analysis of nitrogen pollution across the Yellow River Basin.

2.3. NANI model

The NANI model is a widely adopted framework based on a mass balance approach to quantify the nitrogen inputs to a region that are directly associated with human activities. It provides a comprehensive metric for assessing anthropogenic nitrogen loads at various spatial scales (e.g., regional, basin, or national) and has been extensively used in studies of nutrient cycling, pollution source apportionment, and environmental policy evaluation (Deng et al., 2021; Wang et al., 2022). The NANI framework considers four major components:

$$NANI = N_{im} + N_{fer} + N_{fix} + N_{dep} \quad (1)$$

where *NANI* is the net anthropogenic nitrogen input (kg/(km^2·year)); N_{im} is the nitrogen input of net food or feed (kg/(km^2·year)); N_{fer} is the nitrogen input of fertilizer application (kg/(km^2·year)); N_{fix} is the nitrogen input of crop fixation (kg/(km^2·year)); N_{dep} is the nitrogen input of atmosphere deposition (kg/(km^2·year)).

2.3.1. Net food/feed input

Net food/feed nitrogen input represents the balance between the nitrogen contained in food and feed consumed by the local human and livestock populations and that produced within the region. A positive value indicates a net import of nitrogen—meaning the region imports more food/feed nitrogen than it produces—while a negative value suggests a net export, where food/feed nitrogen is produced in surplus and exported out of the region. The function is as follows:

$$N_{im} = N_{hc} + N_{lc} - N_{lp} - N_{cp} \tag{2}$$

where N_{hc} is the nitrogen content of food consumption by human (kg/(km^2·year)); N_{lc} is the nitrogen content of feed consumption by livestock (kg/(km^2·year)); N_{lp} is the nitrogen content of livestock products (kg/(km^2·year)); N_{lp} is the nitrogen content of crop products(kg/(km^2·year)).

(1) Nitrogen input of human food consumption

$$N_{hc} = (POP_u \times NI_u + POP_r \times NI_r) \times Day \times 10^{-6} / Area \tag{3}$$

where POP_u and POP_r is the urban and rural population (people); NI_u and NI_r is the coefficients of daily nitrogen intake for urban and rural people (mg/(people·day)); Day is the day amount of one year (day); $Area$ is the area of management units (km^2). Parameters are in the Table S1.

(2) Nitrogen input of livestock feed consumption

$$Nlc = \sum_{i=1}^{11} (LA_i \times LI_i) \Big/ Area \tag{4}$$

where i is 11 species of livestock (cattle, cow, pig, sheep, goat, horse, donkey, mule, camel, chicken, duck and goose); LA is the livestock amount (head); LI is the livestock intake coefficient (kg/(head·year)). Parameters are in the Table S2.

(3) Nitrogen output of livestock products

$$N_{lp} = \sum_{i=1}^{11} [LA_i \times (LI_i - LE_i) \times EP_i] \Big/ Area \tag{5}$$

where LE is the livestock excretion coefficient (kg/(head·year)); EP is the edible proportion of livestock products (%). Parameters are in the Table S3 and S4.

(4) Nitrogen output of crop products

$$N_{cp} = \sum_{j=1}^{18} (CY_j \times NC_j \times EP) \Big/ Area \tag{6}$$

where j is the 18 species of crop (Maize, Sorghum, Wheat, Barley, Potatoes, Soybeans, Rice, Groundnut, Sunflower, Cotton, Sugar beet, Olive, Cassava, Vegetables, Pasture and meadow, Crops NES, Other oilseeds, Other cereals); CY is the crop yield (kg/year); NC is the percent of nitrogen content (%). Parameters are in the Table S5.

2.3.2. Fertilizer application input

$$N_{fer} = (NF + CF \times Nr)/Area \tag{7}$$

where NF is the application of nitrogen fertilizer (kg/year, nitrogen equivalent); CF is the application of compound fertilizer (kg/year); Nr is the percent of nitrogen content (%). Parameters are in the Table S6.

2.3.3. Crop fixation input

$$N_{fix} = \sum_{m=1}^{7} (Fix_m \cdot Ar_m) \Big/ Area \tag{8}$$

where m is the 7 species of crop (pulses, soybean, leguminous plants, pasture, paddy, maize/wheat); Fix is the crop nitrogen fixation efficiency (kg/km^2); Ar is the crop planting area (km^2). Parameters are in the Table S7.

2.3.4. Atmospheric deposition input

Atmospheric nitrogen deposition in this study denotes the transfer of reactive nitrogen from the atmosphere to terrestrial ecosystems, which is commonly categorized into oxidized nitrogen and reduced nitrogen, and further subdivided into dry and wet deposition pathways. This study utilizes the gridded atmospheric nitrogen deposition datasets that offer high-resolution spatial estimates suitable for long-term analysis of exogenous nitrogen input from human activities (Gao et al., 2020; Yu et al., 2019). The nitrogen deposition dataset is constructed by integrating multiple existing national-scale gridded data sources, and harmonized into a consistent, continuous time series from 1980 to 2020 through linear interpolation and cross-dataset fusion techniques. This approach ensured temporal completeness and spatial resolution suitable for long-term sub-basin analysis across the Yellow River Basin.

$$N_{dep} = \sum_{cell} (ND_{cell} \cdot Ar_{cell}) \Big/ Area \tag{9}$$

where ND is the cell nitrogen deposition intensity (kg/km^2); Ar is the cell area (km^2).

2.4. Spatial analysis of nitrogen input patterns

The gravity center model is a widely used tool for assessing the spatial distribution and temporal migration patterns of regional attributes. It has been extensively applied in the long-term spatiotemporal evolution analysis of environmental pollution, population distribution, and energy consumption (Guo et al., 2022; Liang et al., 2021). In this study, the model is employed to trace the spatial dynamics of NANI and its four major components across the Yellow River Basin from 1980 to 2020. By analyzing changes in the coordinates of gravity centers and their movement distances, this method captures both the direction and magnitude of nitrogen input shifts.

$$\overline{x}_t^k = \frac{\sum_{i=1}^{n} \left(x_i \cdot w_{i,t}^k\right)}{\sum_{i=1}^{n} w_{i,t}^k}, \quad \overline{y}_t^k = \frac{\sum_{i=1}^{n} \left(y_i \cdot w_{i,t}^k\right)}{\sum_{i=1}^{n} w_{i,t}^k} \tag{10}$$

where x_i and y_i denote the longitude and latitude of grid cell or subregion i; $w_{i,t}^k$ is the value of variable k in year t for region i; and n is the total number of regions.

To quantify the migration of nitrogen input centroids over time, we calculated the great-circle distance between centroid coordinates in successive years using the Haversine formula, which accounts for the Earth's curvature and is widely applied in geospatial analyses:

$$d = 2R \cdot \arcsin\left(\sqrt{\sin^2\left(\frac{\phi_1 - \phi_2}{2}\right) + \cos(\phi_1) \cdot \cos(\phi_2) \cdot \sin^2\left(\frac{\lambda_1 - \lambda_2}{2}\right)}\right) \tag{11}$$

where d is the distance between two centroids (in km), R is the Earth's mean radius (6,371 km), ϕ_1 and ϕ_2 are the latitudes of the two centroids (in radians), λ_1 and λ_2 are the longitudes of the two centroids (in radians). All centroid coordinates were first converted from degrees to radians before computation. This method provides an accurate measurement of displacement trajectories between centroid positions in different years, allowing for robust spatiotemporal analysis of nitrogen input migration patterns.

2.5. Cluster analysis of nitrogen managements

To support the delineation of differentiated nitrogen management zones in the Yellow River Basin, this study employs an unsupervised K-means clustering algorithm to classify all 347 tertiary sub-basins. The

clustering is based on two key indicators: (1) NANI intensity in the year 2020 and (2) the average annual growth rate of NANI from 1980 to 2020. The combination of these two indicators captures both the current state (input level) and the long-term trajectory (change rate) of nitrogen inputs, which are critical for identifying priority zones for differentiated management. Prior to clustering, all input variables are standardized (z-score normalization) to ensure comparability and avoid scale-related biases. The K-means clustering algorithm partitions n observations into k clusters by minimizing the within-cluster sum of squared distances (WCSS). The objective function is defined as follows:

$$SE = \sum_{j=1}^{K} \sum_{x_i \in C_j} \|x_i - \mu_j\|^2 \quad (12)$$

where K is the number of clusters, C_j is the set of sub-basins in cluster j, and μ_i represents the centroid of cluster j. The algorithm iteratively updates cluster assignments and centroids until convergence is achieved or the change in centroids falls below a pre-defined threshold.

To determine the optimal number of clusters, we combined the elbow method with the Calinski–Harabasz (*CH*) Index and silhouette coefficient. The final choice of $k = 9$ captured a meaningful balance between interpretability and model performance, allowing identification of nuanced nitrogen management typologies. The clustering results were visualized using bivariate classification maps, and further interpreted in relation to spatial patterns of fertilizer use, population density, cropland expansion, and proximity to urban centers. This approach enables a more operational and evidence-based delineation of nitrogen control zones compared to conventional administrative or hydrological classifications.

$$CH = \frac{\sum_j n_j \|u_j - u\|^2 / (K-1)}{\sum_j \sum_{x_i \in C_j} \|x_i - u_j\|^2 / (n_j - K)} \quad (13)$$

where n_j is the number of sub-basins in cluster j, μ_j is the centroid of cluster j, μ is the global centroid of all sub-basins.

3. Results and discussion

3.1. Temporal trends and phased evolution

The total nitrogen input exhibits a typically inverted U-shaped trend in the Yellow River Basin from 1980 to 2020. Total inputs increase from 2.48×10^9 kg in 1980 to 5.18×10^9 kg in 2020—an overall growth of approximately 2.09 times, corresponding to an average annual increase of 1.86 % (Fig. 2). Based on temporal patterns, the evolution of NANI can be divided into four distinct phases: a rapid growth phase I (1980–1995) with an annual increase rate of 3.89 %; a moderate growth phase II (1996–2010) with a slowed rate of 1.82 %; a stable phase III (2011–2015) with 5.9×10^9 kg/year; and a decline phase IV (2015–2020), marked by an average annual reduction of −3.01 % (Zheng et al., 2023). In terms of input intensity, NANI rises from 3,079 kg/(km^2·yr) in 1980 to a peak of 7,350 kg/(km^2·yr) in 2013, before decreasing to 6,433 kg/(km^2·yr) by 2020. This trajectory mirrors the national trend in fertilizer consumption, highlighting the pivotal role of agricultural input intensity in shaping nitrogen loads in the basin. Compared to the national average, the Yellow River Basin has consistently exhibited significantly higher NANI intensity (Wang et al., 2024b). For instance, the basin's NANI intensity (4,653 kg/(km2·yr)) in 1990 was 1.37 times the national average (3,400 kg/(km2·yr)), increasing to 1.4 times by 2020 (Han et al., 2014). However, when benchmarked against other N-intensive basins in China, the Yellow River's intensity remains moderate—for example, accounting for only 26.3 % of the Huai River's level in 2010, and 85.0 % and 90.0 % of the Yangtze and Pearl Rivers' levels, respectively, in 2015 (Zhang et al., 2025a; Zhao et al., 2022; Zhong et al., 2022). On a global scale, it is substantially higher than that of typical watersheds in North America and Western Europe. In the early 2000 s, NANI in many major basins along the U.S. East Coast and in Western Europe generally ranged from 2,000 to 4,000 kg/(km^2·yr), well below the 6,000–7,300 kg/(km^2·yr) observed in the Yellow River Basin during the same period (Goyette et al., 2016; Hong et al., 2012; Schaefer and Alber, 2007). This underscores the long-standing nitrogen pressure induced by agricultural intensification and population agglomeration in the basin, which has imposed considerable burdens on ecosystem health. Encouragingly, the post-2015 decline in NANI reflects the preliminary success of national policy interventions, including the "zero growth action plan for fertilizer use", expanded wastewater treatment capacity, and strengthened nitrogen emission regulations (Yu et al., 2025; Zhao et al., 2024). Nonetheless, as of 2020, the input intensity remained 2–3 times higher than those in developed countries, signaling a substantial gap in nitrogen management efficiency (Han et al., 2020; Li et al., 2024a). Moving forward, a coordinated strategy encompassing fertilizer-use efficiency, source reduction, and ecological restoration is urgently needed to reconcile agricultural productivity with ecological sustainability.

The intensity and contribution structure of nitrogen inputs undergo significant changes in the Yellow River Basin from 1980 to 2020. Multi-year average input intensity reveals a highly unbalanced input structure, with chemical fertilizer application (2,753 kg/(km^2·yr)) and food/feed consumption (1,985 kg/(km^2·yr)) dominating the total inputs, while atmospheric nitrogen deposition (808 kg/(km^2·yr)) and biological nitrogen fixation (116 kg/(km^2·yr)) remained relatively low. Fertilizer application emerges as the largest and most variable source. Its unit-area input peaks in 2014 at 4,035 kg/(km^2·yr), and its share of NANI increases from 31.3 % in 1980 to a peak of 55.4 % in 2015, then slightly declines to 52.9 % in 2020-exhibiting a characteristic inverted-U pattern. This trend reflects the substantial regulatory impact of national policies, particularly the "zero growth action plan for fertilizer

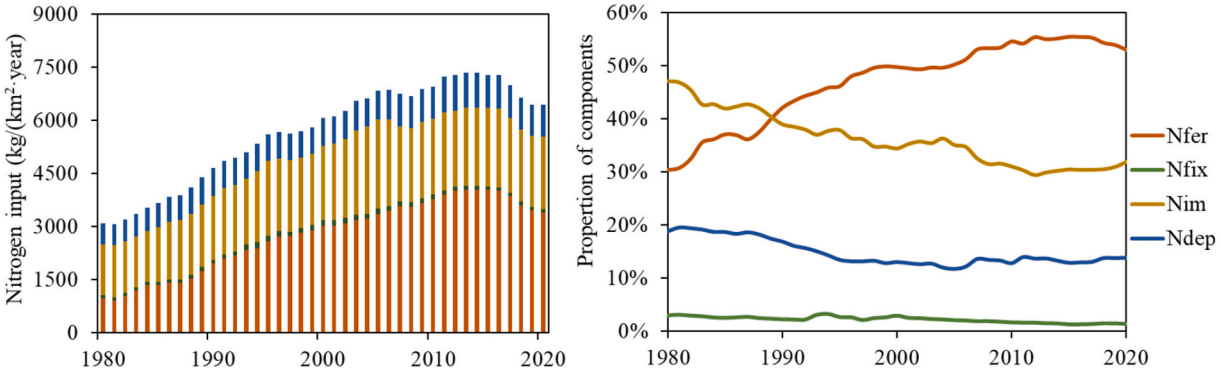

Fig. 2. Temporal changes in net anthropogenic nitrogen input and its components in the Yellow River Basin from 1980 to 2020. (For interpretation of the references to colour in this figure legend, the reader is referred to the web version of this article.)

use" implemented in 2015 (Cheng et al., 2025; Ye et al., 2024). In addition, the intensification of agriculture in the middle and lower reaches of the basin and limited awareness of precision fertilization among farmers, further reinforced the dominance of fertilizer-derived nitrogen (Zhao et al., 2020). Food and feed nitrogen input rank second in contribution. Their intensity peaks in 2005 at 2,534 kg/(km^2·yr) and declined thereafter, with their share of NANI dropping from a high of 47.8 % in 1981 to 31.9 % in 2020. Although urbanization continues to advance, the rapid improvement in domestic wastewater treatment capacity effectively mitigates the pressure from this source (Deng et al., 2025; Zhai et al., 2023). The number of urban wastewater treatment plants in China increases from 70 in 1980 to 2,618 in 2020, with daily treatment capacity rising from 0.7 million to 193 million cubic meters, significantly reducing nitrogen contributions from domestic sources (Bai et al., 2025). Atmospheric deposition exhibits relatively moderate variation, reaching a peak in 2011 and declining gradually thereafter. Its share of NANI decreases from 18.8 % in 1980 to 13.9 % in 2020. This trend closely aligns with reductions in national emissions of nitrogen oxides (NO_x) and ammonia (NH_3) (Yu et al., 2019; Zhang et al., 2025b). From 2011 to 2020, China's annual NO_x emissions drop from 24.03 million tons to 10.19 million tons, while fertilizer use fall from 57.04 million tons to 52.51 million tons, jointly contributing to reduced atmospheric nitrogen deposition (Dentener et al., 2006; Ianniello et al., 2011). Biological nitrogen fixation remains a minor source throughout the study period, with its share decreasing from 2.9 % in 1980 to 1.3 % in 2020. Although its direct contribution to nitrogen budgets is limited, as a key component of ecological agriculture, its role warrants more attention in future sustainable farming practices (Xiao et al., 2024). In summary, the NANI structure has been long dominated by chemical fertilizers and food/feed consumption, which together accounted for over 80 % of total inputs. Among them, chemical fertilizer is the most dynamic and policy-responsive component and remains the primary target for nitrogen pollution control in the basin. While nitrogen inputs from food and feed sources have shown phased mitigation, challenges persist under ongoing population agglomeration. Meanwhile, atmospheric deposition and biological fixation, though less significant in quantity, reflect the long-term feedback mechanisms between agricultural and environmental systems and should continue to be monitored and studied.

3.2. Spatial heterogeneity and inverse growth pattern

To systematically reveal the spatial heterogeneity of nitrogen inputs across the Yellow River Basin, this study develops a hierarchical spatial management framework comprising basin-wide, secondary, and tertiary control units. Using data at five-year intervals from 1980 to 2020, we analyze the spatial distribution patterns and temporal trends of NANI across multiple scales. The proposed zoning approach ensures spatial consistency while facilitating the identification of key regional disparities, thereby supporting targeted, zone-specific management strategies (Liu et al., 2022; Zheng et al., 2023). Overall, NANI intensity in the Yellow River Basin exhibits pronounced spatial differentiation, characterized by a stepwise increase from the upstream to the downstream regions (Fig. 3). This spatial gradient closely corresponds to variations in land use, topography, and population density: the downstream region is predominantly lowland plains with concentrated cropland and dense population; the midstream comprises hilly and mountainous areas with moderate agricultural activities; and the upstream region consists mainly of high-altitude deserts and sparsely populated areas (Tian et al., 2025). As a result, per-area NANI in the downstream is substantially higher than in the upstream, a spatial pattern that aligns closely with the distribution of potential crop yield across China (Liu et al., 2015). In 2020, the control unit with the highest anthropogenic nitrogen input is the main stem of the Yellow River from the Qin River to the estuary,

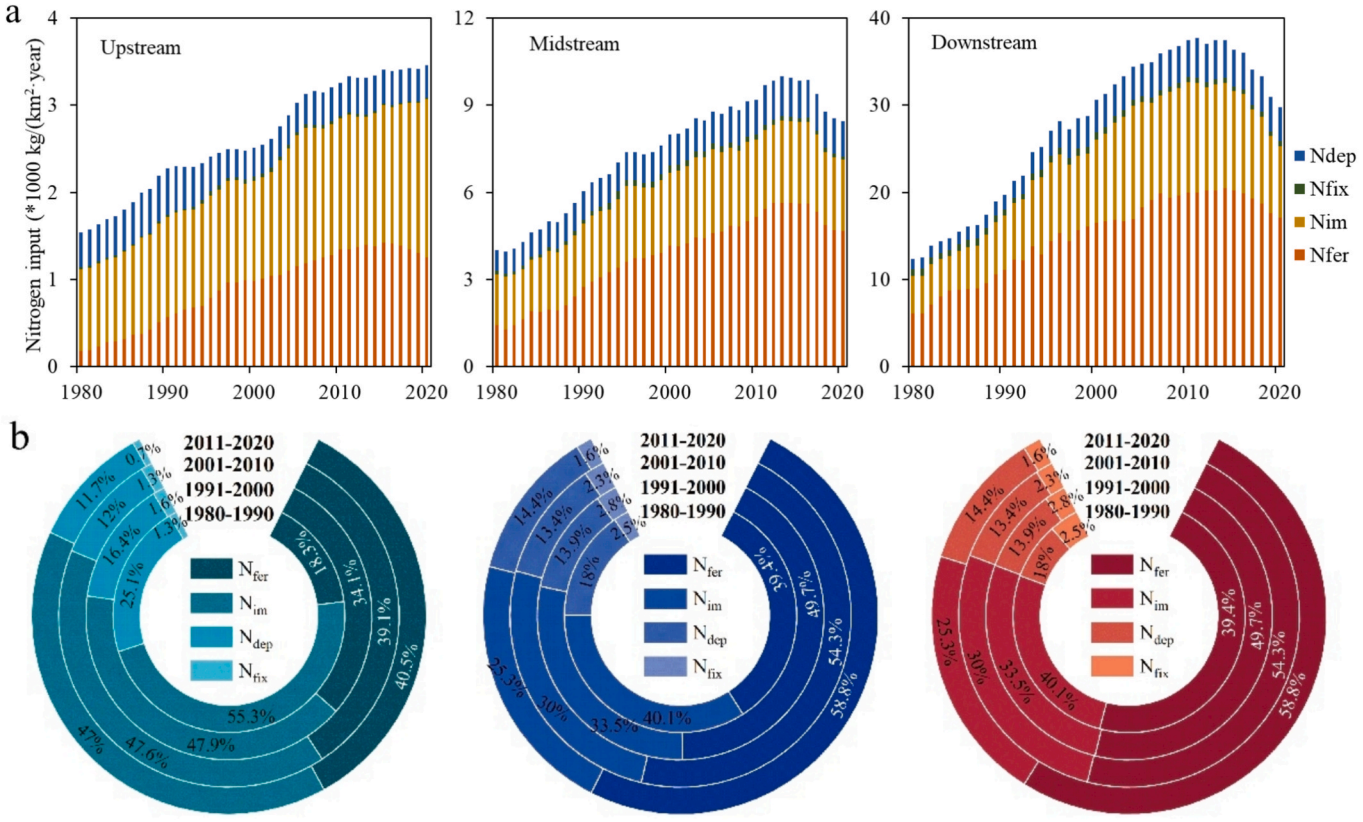

Fig. 3. Temporal variations of net anthropogenic nitrogen input and its components in the upstream, midstream, and downstream regions of the Yellow River Basin from 1980 to 2020. (For interpretation of the references to colour in this figure legend, the reader is referred to the web version of this article.)

reaching 29,291 kg/km^2·a-approximately 4.6 times the basin-wide average. This is followed by the Dawen River sub-basin (21,568 kg/km^2·a) (Zhang et al., 2025a). Areas with medium input intensity are mainly located in the lower reaches below Longyangxia Dam and in agricultural hotspots of the midstream region (Zhou et al., 2023). In contrast, the weakest nitrogen inputs are observed in the source region of the Yellow River up to the Heihe River segment (375 kg/km^2·a) and the internal drainage area of the midstream (736 kg/km^2·a). The NANI intensity between the highest and lowest control units differed by nearly 78-fold, indicating extremely high spatial disparity within the basin. Notably, this spatial structure has remained largely stable over the past four decades, suggesting that anthropogenic nitrogen inputs are predominantly shaped by long-standing land use and socioeconomic patterns. For instance, although the downstream accounts for only 3.7 % of the basin area, it contributes 15.5 % of the NANI in 2020; the midstream, covering 45.8 % of the area, contributed 57.3 %; while the upstream, despite encompassing 50.5 % of the basin, contributed only 27.2 % of NANI. In summary, the spatial distribution of NANI in the Yellow River Basin follows a stable gradient of "high in the downstream, moderate in the midstream, and low in the upstream," with significant disparities and well-defined zonation (Li et al., 2025c). This spatial pattern reflects the combined effects of natural endowments and anthropogenic activities and provides a robust spatial and multi-scale basis for implementing zoned nitrogen control and precision management strategies in the future.

Over the past four decades, nitrogen inputs in the Yellow River Basin increase by 108.9 %. However, the growth rates exhibit a "reverse gradient" pattern—opposite to the spatial distribution of NANI intensity—where regions with initially low nitrogen input have experienced the most rapid increases (Fig. 4). The upstream records the highest growth rate (124.6 %), followed by the downstream (116.1 %), while the midstream shows a relatively lower increase (100.5 %), reflecting a notable rise in nitrogen input in formerly low-NANI areas. In terms of source components, nitrogen from fertilizer application increased most dramatically, by 253 % overall, with regional disparities: 605 % in the upstream, 230 % in the midstream, and 179.4 % in the downstream. In contrast, nitrogen inputs from food/feed imports grow more moderately (41.6 %), yet with marked spatial heterogeneity-92.9 % in the upstream versus only 16.5 % and 19.4 % in the midstream and downstream, respectively. Atmospheric nitrogen deposition increases by 54.1 % overall, with a slight decline in the upstream (−6.5 %) and sharp increases in the midstream (67.2 %) and downstream (228.4 %). Biological nitrogen fixation from crops decrease by 4.83 % overall, with noticeable declines in the upstream (−11.36 %) and downstream (–23.38 %), while the midstream show a slight increase (7.49 %). At the level of secondary management units, the most rapidly growing areas are mainly located in upstream and midstream agricultural expansion zones, including the Wuliangsuhai section of the main stem (298.1 %), the Qingshui River basin (275 %), and the main stem from Qingshui River to Wuliangsuhai (269.8 %). In contrast, the slowest-growing areas are concentrated in the upper headwaters and midstream internal drainage regions, such as the segment from the river source to the Heihe River (0.8 %), the Qu Shui'an to Daxia River segment (14.9 %), and the midstream endorheic zone (15.8 %). At the tertiary sub-basin level, NANI increases in the majority of control units, with only a few exceptions. From a temporal perspective, 1980–1990 marks a period of general increase, especially in agricultural hotspots such as the Hetao Plain and the North China Plain, where NANI in the Wuliangsuhai area rose by 101.6 %. Growth continued from 1990 to 2000, although some plateau regions, including the Qinghai-Tibet and Ordos Plateaus, experience slight declines primarily due to reduced atmospheric nitrogen deposition. Between 2001 and 2010, the upward trend intensified again, with typical regions such as the Dahei River Basin and the section from Wuliangsuhai to Dahei River showing growth rates of 49.7 % and 44.8 %, respectively, from 2001 to 2005. During 2010–2015, trends began to diverge: the downstream region experiences an overall decline (−4.0 %), while the midstream and upstream regions continue to grow modestly (1.6 % and 2.4 %, respectively). The period of 2016–2020 marks a critical turning point, with basin-wide NANI declining overall by 11.5 %, including a 14.8 % drop in the midstream and an 18.8 % decrease in the downstream. This decline is largely driven by a significant reduction in fertilizer nitrogen inputs (−15.4 %), coinciding with the implementation of the "zero growth action plan for fertilizer use" launched by the Ministry of Agriculture in 2013 and the "air pollution

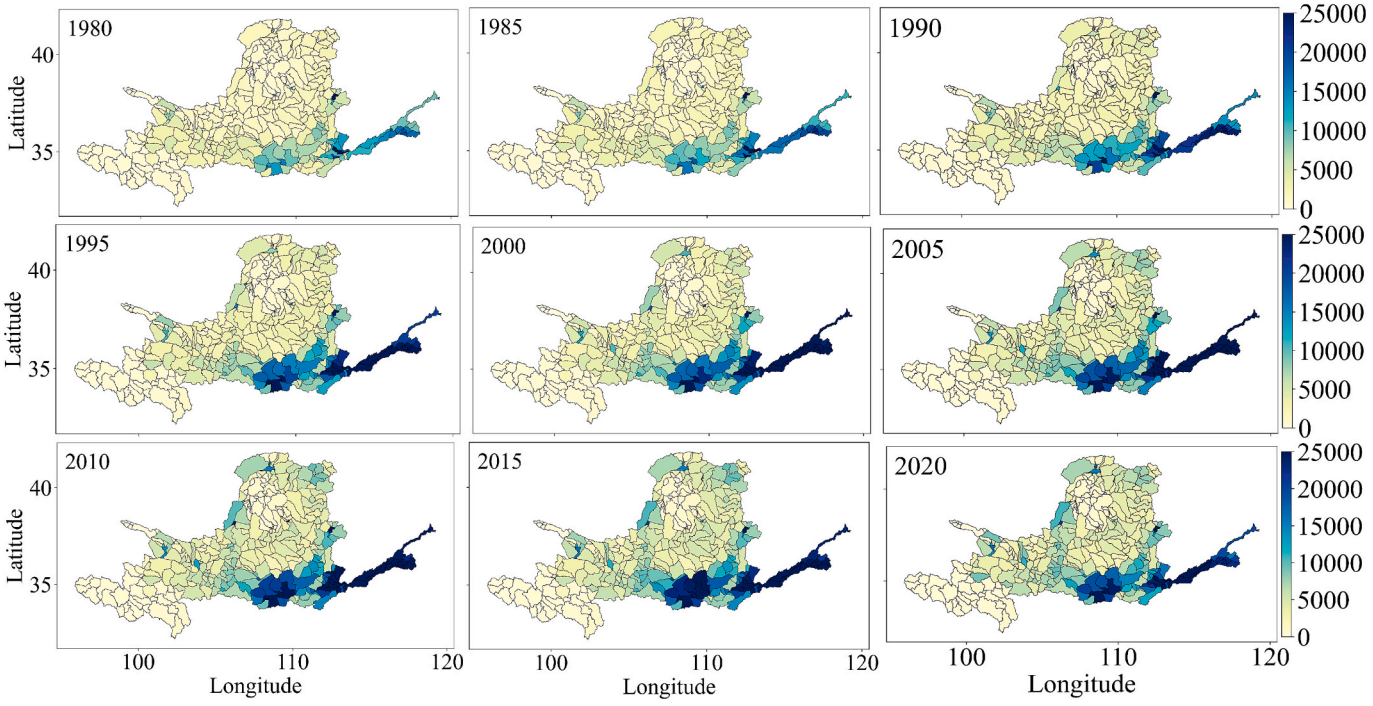

Fig. 4. Spatial distribution of net anthropogenic nitrogen input (kg/(km^2·year)) in the Yellow River Basin at five-year intervals from 1980 to 2020. (For interpretation of the references to colour in this figure legend, the reader is referred to the web version of this article.)

prevention and control action plan," which substantially reduced NO_x emissions and thereby further curbed atmospheric nitrogen deposition (Cheng et al., 2025; Wang, 2025). In summary, NANI in the Yellow River Basin exhibits a reverse spatial expansion pattern—characterized by higher growth rates in initially low-intensity region—and followed a three-phase temporal trajectory: "rapid growth – regional divergence – overall decline." Notably, turning points in NANI dynamics closely align with the timing of national policy interventions, providing critical empirical support for formulating region-specific nitrogen mitigation strategies in the future.

3.3. Dynamic responses of NANI to economic and spatial drivers

A nonlinear relationship between economic development and nitrogen pollution is observed in the Yellow River Basin, with nitrogen inputs first rising and then declining as GDP per capita increased. To interpret this coupling pattern, we apply the environmental kuznets curve (EKC) framework, which focuses on examining the relationship between economic growth and environmental pressures, and is widely used to assess the dynamic interplay between economic growth and environmental pressures (Durmaz and Thompson, 2024). In this study, after comparing alternative model specifications, we selected the segmented regression function for its best-fitting performance and ability to clearly capture distinct development stages. Based on panel data from 1980 to 2020, a segmented regression model is fitted to reveal the turning point of this relationship and explore its regional heterogeneity. The results reveal a typical inverted U-shaped EKC pattern at the basin scale, with an inflection point occurring when per capita GDP reaches approximately 41,000–46,000 CNY (Fig. 5, Fig. 6). During the early stage of economic development (GDP per capita < 15,000 CNY), NANI increases logarithmically with GDP growth, primarily driven by population expansion, intensification of agricultural inputs, and industrialization. In contrast, during the later stage of development (GDP per capita > 40,000 CNY), NANI begins to decline, attributed to green transformation efforts, reductions in fertilizer use intensity, enhanced wastewater treatment capacities, and the declining share of nitrogen-intensive industries (Li et al., 2025b; Wang et al., 2025a). Regional heterogeneity further reveals that the downstream region has completed the full EKC trajectory—characterized by "growth-plateau-decline"-and has already surpassed the turning point, exhibiting a decoupling between economic growth and environmental degradation (Wang et al., 2025b; Zhang et al., 2024b). These regions should now focus on consolidating reductions, preventing rebound effects, and serving as demonstration zones for low-N development. In contrast, the upstream remains on the rising segment of the EKC, with lower per capita GDP and continued pressure on nitrogen inputs from agriculture and population, showing no clear turning point in nitrogen reduction. These regions require early policy entry points to prevent long-term pollution lock-in, especially through ecological redlines, agricultural land-use planning, and investment in early-stage nutrient monitoring infrastructure. The spatial divergence in EKC trajectories has been confirmed by numerous studies, underscoring that pollution control and economic growth do not evolve synchronously but are instead shaped by a complex interplay of resource endowments, governance capacity, and policy implementation (Mutascu, 2025; Ozturk et al., 2024). More importantly, the EKC trajectory in the Yellow River Basin has been shaped not by spontaneous market adjustments but by a series of targeted interventions—including total pollutant control systems, green agriculture promotion, and region-specific development strategies (Cui et al., 2024; Zhang et al., 2024a). The emergence of EKC turning point is thus a consequence of the combined effects of institutional pressure and technological progress. Without sustained policy support and continuous innovation, the current downward trend in NANI could stagnate or even reverse. This finding highlights the critical importance of building long-term, stable mechanisms for green development to consolidate and expand nitrogen reduction achievements in the basin.

The geographic shift of nitrogen input centroids serves as a critical indicator of agricultural expansion, pollution redistribution, and the spatial evolution of socioeconomic activities. This study is the first to apply a centroid trajectory analysis at the scale of the Yellow River Basin to systematically assess the five-year spatial dynamics of total nitrogen input and its four major sources—fertilizer application, food/feed nitrogen, atmospheric deposition, and biological nitrogen fixation—over the period 1980–2020 (Fig. 7). Overall, the centroids of NANI and its

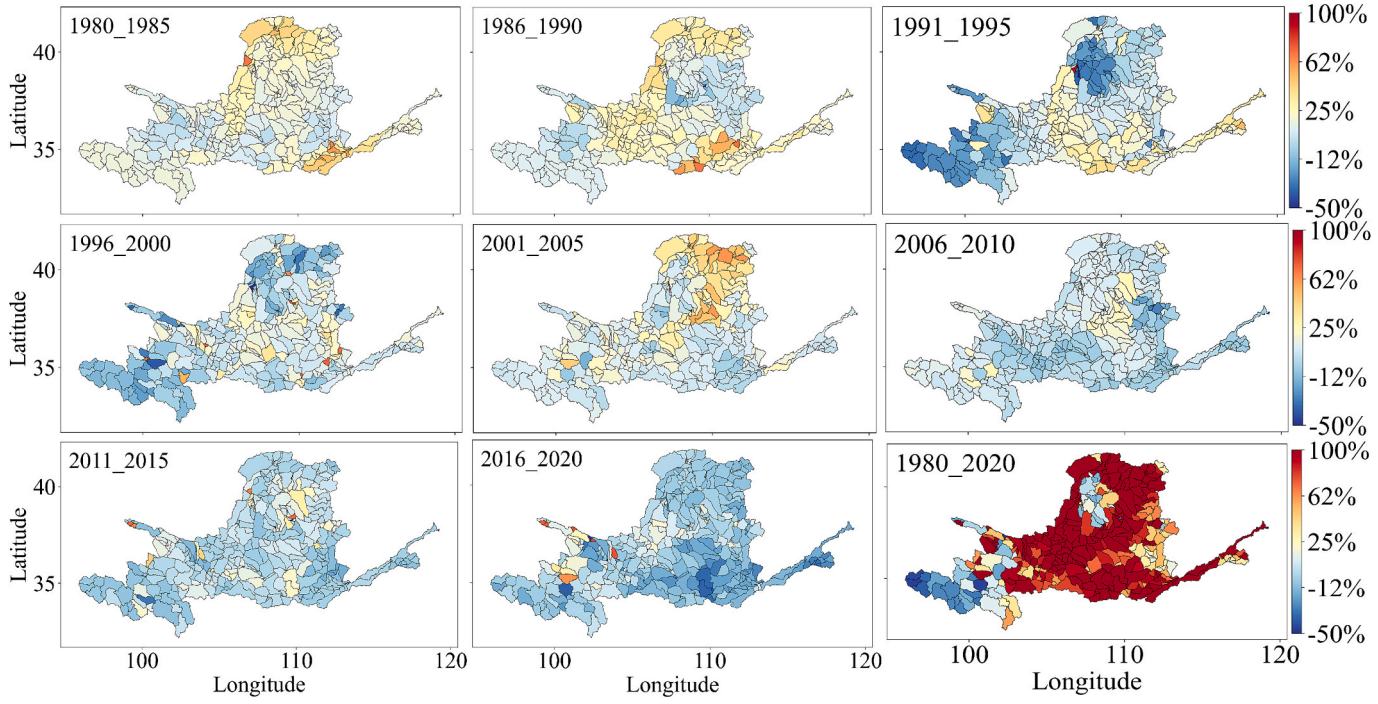

Fig. 5. Changes in the five-year growth rate of net anthropogenic nitrogen input in the Yellow River Basin from 1980 to 2020. (For interpretation of the references to colour in this figure legend, the reader is referred to the web version of this article.)

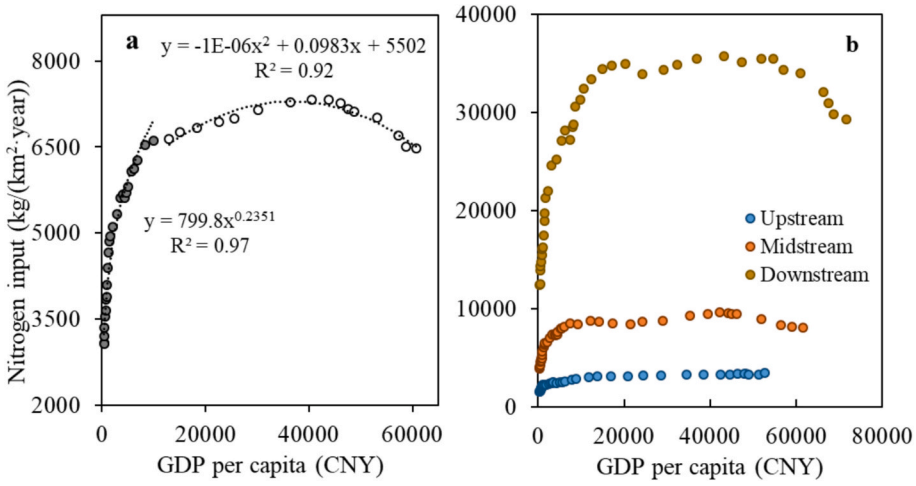

Fig. 6. Relationship between net anthropogenic nitrogen input and per capita GDP in the Yellow River Basin (a) and its upstream, midstream, and downstream regions (b) from 1980 to 2020. (For interpretation of the references to colour in this figure legend, the reader is referred to the web version of this article.)

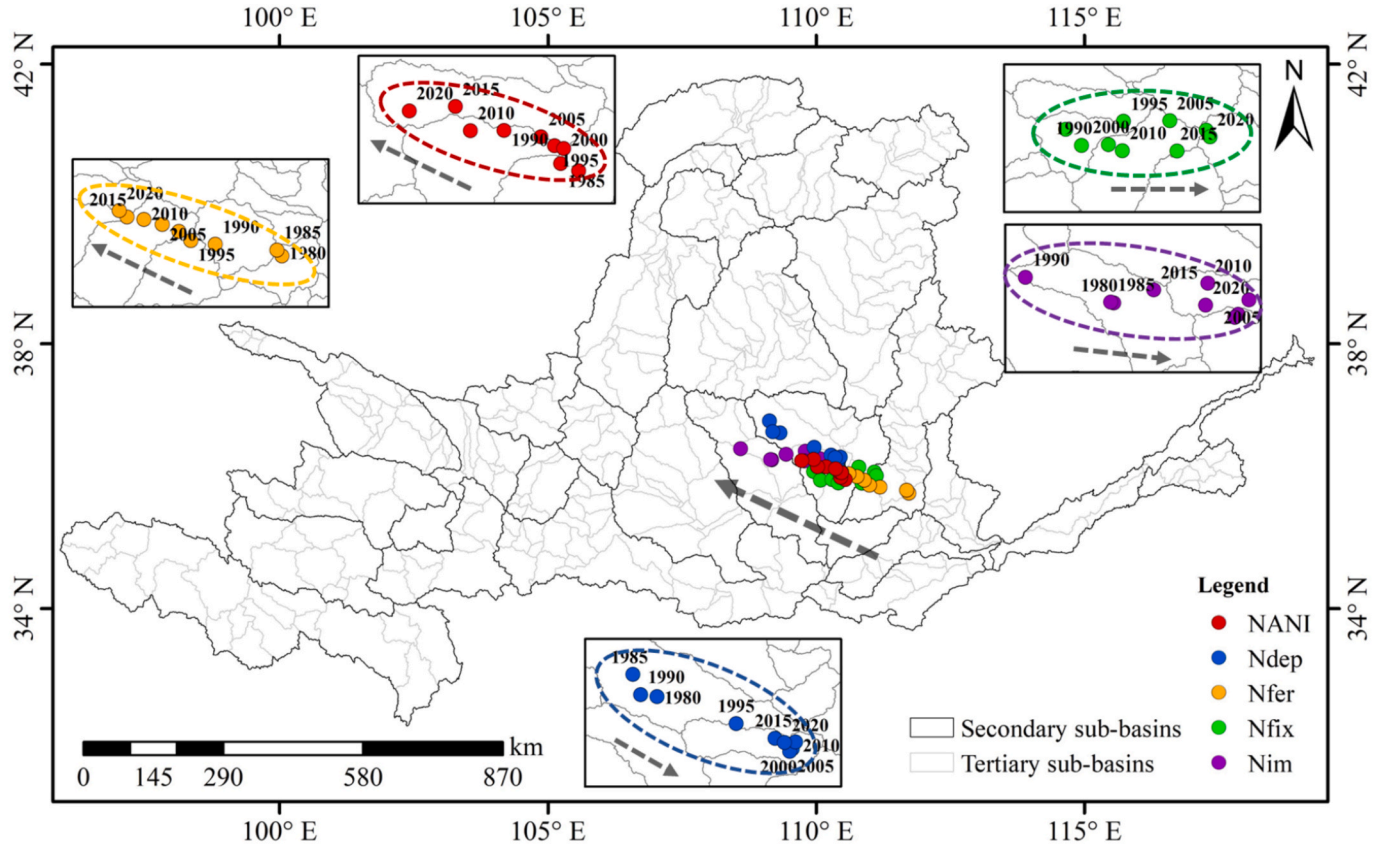

Fig. 7. Temporal dynamics of spatial centroids for net anthropogenic nitrogen input and its components in the Yellow River Basin from 1980 to 2020. (For interpretation of the references to colour in this figure legend, the reader is referred to the web version of this article.)

major components remained consistently concentrated near the midstream region, particularly around the Shanxi-Shaanxi junctions, forming an elliptical agglomeration belt extending in a northwest-southeast direction (He et al., 2025; Liu et al., 2025). From 1980 to 2000, the centroids exhibit a persistent southeastward shift, reflecting the strong gravitational pull of agricultural and industrial intensification in the middle and lower reaches. After 2000, however, the centroid begins to migrate northwestward, with a total displacement of 73.73 km at an average annual rate of approximately 3.69 km, peaking during 2016–2020 with a single-period movement of 34.57 km. This spatial turning point coincides with the launch of the "Western Development Strategy" and reflects increasing nitrogen input intensity in western regions (Dai et al., 2022; Zheng et al., 2022). Source-specific analysis reveals substantial heterogeneity in centroid migration trajectories: (1) Fertilizer-derived nitrogen exhibits a steady southeast-to-northwest shift, with a total displacement of 237.66 km over 40 years. Moreover, the spatial trajectory of fertilizer nitrogen closely mirrors that of total anthropogenic nitrogen input: the correlation coefficients between their centroid coordinates are 0.98 for longitude and 0.88 for latitude, respectively. This high degree of alignment indicates that agricultural

planting activities, particularly fertilizer application, are the dominant driver of anthropogenic nitrogen input dynamics across the basin. This trend highlights the intensifying fertilizer use in northwestern agricultural zones and underscores the urgent need for enhanced nutrient management and fertilizer reduction strategies in these areas (Yang et al., 2024). (2) Food/feed nitrogen shows a west-to-east migration between 1980 and 2005, indicating a concentration of domestic-source nitrogen pollution in downstream urban areas during rapid urbanization. After 2005, the centroid partially shifted back westward, suggesting emerging pollution pressures from livestock production and small to medium-sized cities in the western regions (Yang et al., 2023). (3) Atmospheric nitrogen deposition experiences an initial northwest-to-southeast migration, followed by a slight reversal (total movement of 161.51 km). This pattern may reflect the initial effectiveness of emission control policies in eastern China, while highlighting increasing atmospheric nitrogen burdens in central and western regions (Tian et al., 2025). (4) Biological nitrogen fixation displays no clear directional trend but shows pronounced periodic fluctuations, averaging 42.91 km per interval. These variations are likely driven by shifts in cropping structures and arable land distribution. Previous studies have shown that westward shifts in China's agricultural nitrogen flow are often influenced by institutional interventions such as ecological restoration, cropland retirement in urbanizing regions, and structural adjustments in agriculture (Fu et al., 2024; Li et al., 2025b). As a national ecological protection priority, the Yellow River Basin's shifting nitrogen input centroid reflects deep structural changes in the spatial distribution of human activities. More importantly, it suggests that future pollution control efforts should increasingly focus on ecologically sensitive western subregions, enabling targeted regulation and regionally coordinated nitrogen management strategies.

3.4. Spatial typologies of nitrogen input for tiered management

To support zoned and targeted nitrogen pollution control in the Yellow River Basin, this study employs an unsupervised K-means clustering algorithm to classify all tertiary sub-basins based on two indicators: NANI intensity in 2020 and the growth rate of NANI from 1980 to 2020. This approach effectively integrates multidimensional data while avoiding subjectivity associated with threshold-based classifications, thereby enhancing the objectivity and spatial specificity of nitrogen control unit delineation. The clustering results identify nine composite types of sub-basins, corresponding to combinations of nitrogen input intensity and growth rate-namely, "High-High (H-H)," "High-Medium (H-M)," "High-Low (H-L)," "Medium-High (M−H)," and so on-establishing a differentiated nitrogen input management zoning system based on the dual dimensions of intensity and growth (Fig. 8). Spatial analysis reveals that NANI in the basin exhibits strong spatial clustering and autocorrelation, indicating that nitrogen inputs are not only driven by local agricultural activities and population density, but also influenced by spillover effects from adjacent urban expansion, wastewater discharge, and regional policy dynamics (Sun et al., 2020; Zheng et al., 2023). Specifically, H-H sub-basins are concentrated in tributaries such as the Weihe, Qinhe, Yiluo, and Dawen Rivers, which serve as key agricultural hinterlands for major urban agglomerations including Xi'an, Zhengzhou, Jinan, and Luoyang (Ji et al., 2024; Tian et al., 2025). These regions face dual pressures from intensive fertilizer application and domestic nitrogen sources, making them "core risk zones" for nitrogen pollution. Comprehensive strategies are urgently needed, including fertilizer reduction and substitution, enhanced wastewater nitrogen removal, and rural non-point source control, along with the establishment of coordinated regional governance mechanisms to

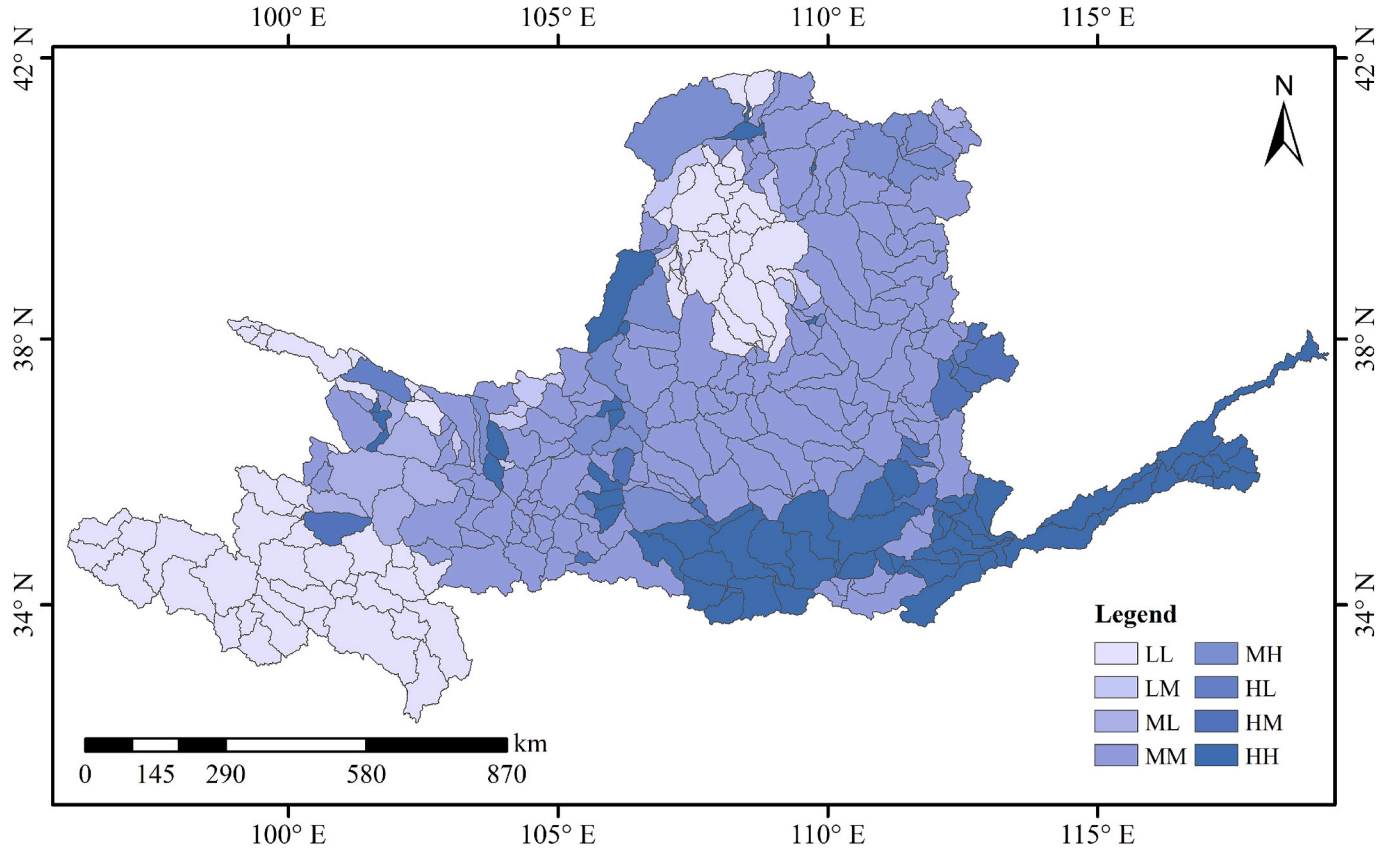

Fig. 8. Spatial classification of tertiary sub-basins in the Yellow River Basin based on NANI intensity in 2020 and historical growth trends (L-L: low NANI and low growth; L-M: low NANI and medium growth; M−L: medium NANI and low growth; M−M: medium NANI and medium growth; M−H: medium NANI and high growth; H-L: high NANI and low growth; H-M: high NANI and medium growth; H-H: high NANI and high growth). (For interpretation of the references to colour in this figure legend, the reader is referred to the web version of this article.)

improve mitigation efficiency and joint prevention capabilities. In contrast, H-L and H-M sub-basins exhibit high input intensities but slower or stable growth trends, suggesting that existing control measures are beginning to show results. These areas should focus on consolidating current achievements and preventing rebound effects. Moreover, they offer valuable opportunities to serve as demonstration zones for medium- to long-term nitrogen control, promoting best practices such as precision fertilization, green cropping systems, and organic substitution. M−H sub-basins, located mainly in the agriculturally suitable midstream and irrigated farming expansion zones, have experienced rapid NANI growth in recent years due to increased grain production and the spread of intensive agriculture. These are designated as "early-warning zones" and should be targeted with timely interventions to prevent transition into high-load areas. M−M and M−L sub-basins show moderate loads and should adopt development-compatible constraint strategies based on their potential risk. Of particular concern are L-H sub-basins, which are primarily distributed along the margins of the Qinghai-Tibet Plateau and the Ordos Plateau-ecologically sensitive regions where current nitrogen inputs remain low but are increasing rapidly (Li et al., 2024b). This trend reflects westward agricultural expansion and growing external pressure on ecological buffer zones. Without timely intervention, these areas could evolve into emerging pollution hotspots. Hence, they should be designated as "ecological early-warning zones," with strict control over nitrogen input sources, farmland expansion, and high-intensity projects (Huang et al., 2022). L-L sub-basins, located in headwater regions, alpine zones, or internal drainage areas, maintain persistently low nitrogen input levels and function as "ecological bottom-line zones" for basin-wide security (Feng et al., 2024). These areas require sustained protection efforts, strict enforcement of ecological redline policies, and restrictions on anthropogenic disturbances. Compared to conventional classifications based on administrative boundaries or hydrological units, the K-means clustering framework proposed in this study offers a more scientific and operationally feasible approach. It not only captures the spatial variation and temporal evolution of NANI but also provides a robust foundation for implementing differentiated control strategies. Based on the clustering results, we propose a multi-tiered management framework tailored to the specific nitrogen input profiles of the Yellow River Basin: (1) For H–H and M−H zones, which are typically concentrated in intensively cultivated and densely populated areas (e.g., Weihe, Yiluo, and Dawen sub-basins), we recommend establishing nitrogen control priority zones. These regions require integrated mitigation strategies targeting agricultural nutrient reduction, enhanced wastewater treatment, and industrial source control, along with strengthened inter-jurisdictional coordination mechanisms; (2) For L-H zones, often located at the ecological margins of the Qinghai-Tibet Plateau and Ordos Plateau, we suggest designating them as early-warning control zones. These areas, though currently low in N load, are experiencing rapid growth due to land conversion and new agricultural projects. Management should emphasize ecological redline protection, regulation of farmland expansion, and proactive control of nitrogen-intensive development; (3) For transitional zones such as M−M and H-M, which show moderate or stabilizing trends in nitrogen inputs, we recommend adopting flexible and adaptive management approaches. These should include ongoing evaluation of development–pollution trade-offs, pilot projects for green agriculture, and the gradual introduction of differentiated fertilizer pricing or quota mechanisms; (4) For L-L zones, mainly located in headwaters, alpine zones, and internal drainage areas, we propose maintaining them as ecological bottom-line protection zones. Management in these areas should focus on long-term ecological monitoring, land use restrictions, and the prevention of anthropogenic disturbances to safeguard the basin's overall nitrogen balance. In summary, the K-means clustering approach offers a scientifically grounded and practically oriented framework for spatially explicit nitrogen management. Under the broader context of China's "dual carbon" goals and the "Beautiful China" initiative, this method helps clarify nitrogen control priorities in the Yellow River Basin and supports the formulation of differentiated, regionally coordinated, and ecologically oriented nitrogen mitigation pathways.

3.5. Limitation and uncertainty

Despite the incorporation of high-resolution spatiotemporal data and a robust methodological framework, the estimation of net anthropogenic nitrogen input and its spatiotemporal dynamics in the Yellow River Basin inevitably involves multiple sources of uncertainty. These uncertainties stem from data quality, parameter assumptions, model structure, and socio-political variability. (1) Data accuracy and consistency represent a core source of uncertainty in NANI estimation. The four major components of NANI—fertilizer application, food/feed nitrogen inputs, atmospheric nitrogen deposition, and biological nitrogen fixation-are derived from multiple data sources, including statistical yearbooks, remote sensing interpretation, model outputs, and literature-based coefficients. Fertilizer data, typically obtained at the county level, often suffer from mismatches between production and application locations, especially near basin boundaries. In addition, the reconstruction of missing historical data, particularly for the period prior to the 1990 s, introduces further uncertainty, as it relies on proportional estimation methods based on limited or aggregated records. Food/feed nitrogen estimates are influenced by shifting population dynamics and changing urban–rural classification criteria, which can compromise temporal consistency. Atmospheric deposition estimates, especially before 2000, are modeled with limited ground observation support, leading to large uncertainty bounds. Biological nitrogen fixation depends heavily on crop types and cropping patterns, and is particularly challenging to estimate in irrigated or reforested areas, where land cover frequently changes. (2) Methodological choices also introduce structural uncertainty. Some key coefficients (e.g., per capita food nitrogen input, livestock excretion rates) assumed constant over time and space, potentially underestimating local heterogeneity or intensification effects. Moreover, to convert nitrogen input data from administrative units to hydrologically defined tertiary sub-basins, we applied proportional downscaling using weighting factors such as population, GDP, and agricultural land area. While this approach is widely used and facilitates alignment with ecological management units, it may introduce spatial allocation errors—especially in regions with mixed land use, cross-boundary cities, or rapidly changing socio-economic conditions. (3) There is a lag between socioeconomic behavior and policy effectiveness. While EKC analysis shows a turning point in nitrogen input trends, this is not an automatic function of economic growth, but the result of policy-driven interventions. Fertilizer reduction, livestock restrictions, and straw return programs are unevenly implemented across regions. (4) The physical and ecological context of the YRB introduces specific challenges. The Yellow River is one of the most regulated river systems globally, with extensive reservoir cascades and inter-basin transfers (Li et al., 2025a; Yarleque et al., 2024). These infrastructures alter nitrogen fate through sedimentation, denitrification, and hydrological attenuation, potentially decoupling NANI values from observed water quality outcomes (Mu et al., 2024; Tian et al., 2025). High nitrogen input in downstream sub-basins, for instance, may be attenuated by reservoir retention before reaching sensitive aquatic ecosystems. Similarly, the basin's high sediment load affects nitrogen through adsorption–desorption processes not accounted for in the NANI model. In addition, the extreme seasonal variation in runoff (with 60 % of annual discharge occurring in 3–4 months) creates temporal mismatches between nitrogen loading and transport, while water scarcity in the lower reaches may exacerbate accumulation and hotspot formation (Dou et al., 2025; Xie et al., 2025). (5) The NANI model, as a pressure-based framework, quantifies potential rather than actual nitrogen export or impact. It does not incorporate retention, transformation, or ecosystem response processes. Nor does it disaggregate the marginal contributions of overlapping drivers such as policy reform, market dynamics, and

climate change. In conclusion, although the NANI estimates in this study provide critical insights into nitrogen input dynamics and priority areas for management, they must be interpreted in light of the basin's hydrological modifications, sediment context, and implementation variability. Future research should consider coupling NANI outputs with hydrological-biogeochemical models, expanding in situ validation efforts, and integrating feedback mechanisms to support more accurate and policy-relevant nitrogen risk assessments in complex basins such as the Yellow River

4. Conclusion

This study presents a comprehensive assessment of the spatiotemporal patterns and driving mechanisms of net anthropogenic nitrogen input in the Yellow River Basin from 1980 to 2020, integrating high-resolution spatial datasets, multi-source nitrogen input accounting, and multiple analytical frameworks including centroid migration, EKC and unsupervised clustering. The results reveal that: (1) Long-term growth with spatial polarization. Over the past four decades, the NANI increased by 108.9 %, but spatial disparity widened significantly. The downstream regions consistently exhibit the highest input intensity, whereas upstream areas experienced the fastest growth, forming a reverse gradient between the baselines and growth rates. (2) Stable spatial hierarchy with shifting frontiers. Although NANI intensity followed a persistent "high downstream-moderate midstream-low upstream" pattern, the centroid and its major sources migrated northwestward after 2000, indicating a spatial frontier of transition driven by agricultural expansion and shifting pollution pressures. (3) Nonlinear coupling with economic growth. A clear EKC relationship was identified, with a per capita GDP threshold (41,000–46,000 CNY) marking the onset of nitrogen decoupling in mid- and downstream regions. Upstream zones remain on the rising curve, reflecting a socioeconomic frontier of transition. (4) Zoned typologies for precision management. K-means clustering classified sub-basins into nine types, corresponding to different nitrogen dynamics and control strategies. These typologies delineate governance frontiers, from priority risk zones to ecological bottom lines.

This study demonstrates the value of identifying spatiotemporal and socioeconomic frontiers of nitrogen pollution to guide more adaptive and region-specific management strategies. By capturing centroid migration patterns, nonlinear economic linkages, and sub-basin clustering typologies, we reveal where and how nitrogen input dynamics are transitioning across the Yellow River Basin. These findings enable the construction of a differentiated management framework aligned with ecological risk, development stage, and policy capacity. More broadly, this research exemplifies how high-resolution, data-driven diagnostics can strengthen basin-scale environmental governance in rapidly developing, resource-constrained regions. Continued integration of nitrogen output pathways and ecosystem responses will be critical for informing long-term sustainable transitions.

CRediT authorship contribution statement

Jincheng Li: Writing – original draft, Methodology, Formal analysis, Data curation. **Zhonghua Li:** Writing – review & editing, Project administration. **Qiang Wang:** Data curation. **Yan Chen:** Writing – review & editing, Project administration. **Xinyue Zhang:** Data curation. **Taher Kahil:** Writing – review & editing. **Dor Fridman:** Writing – review & editing.

Declaration of competing interest

The authors declare that they have no known competing financial interests or personal relationships that could have appeared to influence the work reported in this paper.

Acknowledgments

This research has been supported by the Young Scientists Fund of the National Natural Science Foundation of China (Grant No. 4240707), Beijing Natural Science Foundation (Grant No. 8244067) and National Key Research and Development Program of China (Grant No. 2024YFD1701300).

Appendix A. Supplementary data

Supplementary data to this article can be found online at https://doi.org/10.1016/j.ecolind.2025.114066.

Data availability

Data will be made available on request.

References

Bai, Y., Xu, A., Wu, Y.H., Xue, S., Chen, Z., Hu, H.Y., 2025. Portrait of municipal wastewater of China: Inspirations for wastewater collection, treatment and management. Water Res. 277.

Cai, W.J., Hu, X.P., Huang, W.J., Murrell, M.C., Lehrter, J.C., Lohrenz, S.E., Chou, W.C., Zhai, W.D., Hollibaugh, J.T., Wang, Y.C., Zhao, P.S., Guo, X.H., Gundersen, K., Dai, M.H., Gong, G.C., 2011. Acidification of subsurface coastal waters enhanced by eutrophication. Nat. Geosci. 4, 766–770.

Chellaiah, C., Anbalagan, S., Swaminathan, D., Chowdhury, S., Kadhila, T., Shopati, A.K., Shangdiar, S., Sharma, B., Amesho, K.T.T., 2024. Integrating deep learning techniques for effective river water quality monitoring and management. J. Environ. Manage. 370.

Chen, B.H., Ren, C.C., Wang, C., Duan, J.K., Reis, S., Gu, B.J., 2023. Driving forces of nitrogen use efficiency in chinese croplands on county scale. Environ. Pollut. 316.

Chen, D.J., Shen, H., Hu, M.P., Wang, J.H., Zhang, Y.F., Dahlgren, R.A., 2018. Legacy nutrient dynamics at the watershed scale: principles, modeling, and implications. Adv. Agron. 149 (149), 237–313.

Chen, L., Pu, Y., Zhu, K.H., Guo, C.X., Wang, Y.W., Shen, Z.Y., 2024a. Integrating best management practices with dynamic water environmental capacity for optimal watershed management. J. Environ. Manage. 371.

Chen, L., Yu, W., Zhang, X.B., 2024b. Spatio-temporal patterns of high-quality urbanization development under water resource constraints and their key Drivers: a case study in the Yellow River Basin. China, Ecol Indic, p. 166.

Chen, W.X., Zeng, J., Li, N., 2021. Change in land-use structure due to urbanisation in China. J. Clean. Prod. 321.

Cheng, Z.Q., Zhu, M.Z., Cai, J.Y., 2025. Reducing fertilizer and pesticide application through mandatory agri-environmental regulation: insights from "two zero" policy in china. Environ Impact Asses 110.

Cui, Y.F., Li, L., Lei, Y.L., Wu, S.M., 2024. The performance and influencing factors of high-quality development of resource-based cities in the Yellow River basin under reducing pollution and carbon emissions constraints. Resour. Policy 88.

Dai, J., Zhuo, Y.T., Liao, Z.J., Wen, H.D., 2022. The direction choice of green technological progress and late-development advantage in central and Western China. Heliyon 8.

Deng, C.N., Liu, L.S., Peng, D.Z., Li, H.S., Zhao, Z.Y., Lyu, C.J., Zhang, Z.Q., 2021. Net anthropogenic nitrogen and phosphorus inputs in the Yangtze River economic belt: spatiotemporal dynamics, attribution analysis, and diversity management. J. Hydrol. 597.

Deng, O.P., Wei, J.L., Cui, J.L., Huang, S., Cheng, L.X., Huang, R., Gu, B.J., 2025. Food-driven transformation of nitrogen fluxes with urbanization in China. Resour. Conserv. Recy. 214.

Dentener, F., Drevet, J., Lamarque, J.F., Bey, I., Eickhout, B., Fiore, A.M., Hauglustaine, D., Horowitz, L.W., Krol, M., Kulshrestha, U.C., Lawrence, M., Galy-Lacaux, C., Rast, S., Shindell, D., Stevenson, D., Van Noije, T., Atherton, C., Bell, N., Bergman, D., Butler, T., Cofala, J., Collins, B., Doherty, R., Ellingsen, K., Galloway, J., Gauss, M., Montanaro, V., Müller, J.F., Pitari, G., Rodriguez, J., Sanderson, M., Solmon, F., Strahan, S., Schultz, M., Sudo, K., Szopa, S., Wild, O., 2006. Nitrogen and sulfur deposition on regional and global scales: A multimodel evaluation. Global Biogeochem Cy 20.

Dou, J.H., Xia, R., Xia, X.H., Jiang, X.H., Zhang, K., Chen, Y., Li, L.N., Yan, C., 2025. Extreme rainfall drives the shift in dominant water quality "Sink" from forest land to grassland in the Yellow River Basin. J. Hydrol. 658.

Durmaz, N., Thompson, A., 2024. An environmental kuznets curve for water pollution: does water abundance affect the turning point? Sci. Total Environ. 913.

Feng, Z.W., Yang, X.L., Li, S.B., 2024. new insights of eco-environmental vulnerability in china's yellow river basin: spatio-temporal pattern and contributor identification. Ecol. Ind. 167.

Fu, H., Xie, X., Zhao, K., Chen, D.J., Hu, S.Y., Li, Y.H., Tang, S.J., Shi, L., 2024. Tracking social-economic system nitrogen flow in China for emissions reduction and efficiency improvement. Resour Conserv Recy 207.

Gao, Y., Zhou, F., Ciais, P., Miao, C.Y., Yang, T., Jia, Y.L., Zhou, X.D., Klaus, B.B., Yang, T. T., Yu, G.R., 2020. Human activities aggravate nitrogen-deposition pollution to inland water over china. Natl. Sci. Rev. 7, 430–440.
Goyette, J.O., Bennett, E.M., Howarth, R.W., Maranger, R., 2016. Changes in anthropogenic nitrogen and phosphorus inputs to the St. Lawrence sub-basin over 110 years and impacts on riverine export. Global Biogeochem Cy 30, 1000–1014.
Guo, K., Cao, Y., Wang, Z., Li, Z., 2022. Urban and industrial environmental pollution control in China: an analysis of capital input, efficiency and influencing factors. J. Environ. Manage. 316, 115198.
Han, Y.G., Fan, Y.T., Yang, P.L., Wang, X.X., Wang, Y.J., Tian, J.X., Xu, L., Wang, C.Z., 2014. Net anthropogenic nitrogen inputs (NANI) index application in mainland china. Geoderma 213, 87–94.
Han, Y.G., Feng, G., Swaney, D.P., Dentener, F., Koeble, R., Ouyang, Y., Gao, W., 2020. Global and regional estimation of net anthropogenic nitrogen inputs (NANI). Geoderma 361.
He, J., Tang, Y.F., Guo, X.Q., Chen, H.T., Guo, W., Sun, Y.C., 2025. Assessment of coupling coordination and spatial distribution characteristics between urbanization and ecosystem health in the Yellow River Basin. Land Use Policy 154.
Hong, B., Swaney, D.P., Mörth, C.M., Smedberg, E., Hägg, H.E., Humborg, C., Howarth, R.W., Bouraoui, F., 2012. Evaluating regional variation of net anthropogenic nitrogen and phosphorus inputs (NANI/NAPI), major drivers, nutrient retention pattern and management implications in the multinational areas of Baltic Sea basin. Ecol. Model. 227, 117–135.
Howarth, R.W., Billen, G., Swaney, D., Townsend, A., Jaworski, N., Lajtha, K., Downing, J.A., Elmgren, R., Caraco, N., Jordan, T., Berendse, F., Freney, J., Kudeyarov, V., Murdoch, P., Zhu, Z.L., 1996. Regional nitrogen budgets and riverine N&P fluxes for the drainages to the north atlantic ocean: natural and human influences. Biogeochemistry 35, 75–139.
Huang, L.Y., Wang, J., Chen, X.J., 2022. Ecological infrastructure planning of large river basin to promote nature conservation and ecosystem functions. J. Environ. Manage. 306.
Huang, S.W., Li, H.M., Wang, M.R., Qian, Y.Y., Steenland, K., Caudle, W.M., Liu, Y., Sarnat, J., Papatheodorou, S., Shi, L.H., 2021. Long-term exposure to nitrogen dioxide and mortality: a systematic review and meta-analysis. Sci. Total Environ. 776.
Huo, S.L., Ma, C.Z., Li, W.P., He, Z.S., Zhang, H.X., Yu, L., Liu, Y., Cao, X.H., Wu, F.C., 2022. Spatiotemporal differences in riverine nitrogen and phosphorus fluxes and associated drivers across China from 1980 to 2018. Chemosphere 310.
Ianniello, A., Spataro, F., Esposito, G., Allegrini, I., Hu, M., Zhu, T., 2011. Chemical characteristics of inorganic ammonium salts in PM in the atmosphere of Beijing (China). Atmos. Chem. Phys. 11, 10803–10822.
Ji, Q.L., Feng, X.M., Zhang, J.Z., Fu, B.J., 2024. Uncovering leveraging and hindering factors in socio-ecological interactions: agricultural production in the yellow river basin as an example. J. Environ. Manage. 368.
Lai, X.M., Zhu, Q., Castellano, M.J., Liao, K.H., 2022. Soil rock fragments: unquantified players in terrestrial carbon and nitrogen cycles. Geoderma 406.
Lai, Z.C., Li, L., Huang, M., Tao, Z.M., Shi, X.T., Li, T., 2024. Spatiotemporal evolution and decoupling effects of sustainable water resources utilization in the yellow river basin: based on three-dimensional water ecological footprint. J. Environ. Manage. 366.
Li, D.L., Li, J.Y., Wang, Y.J., Jiang, E.H., Zhao, W.J., Liu, G., Yang, Z.F., 2025a. A multi-attribute decision-making method of cascade reservoir joint scheduling schemes considering water-sediment, eco-environment, and socio-economy in the yellow river basin. J. Hydrol. 660.
Li, J.C., Fu, J.X., Kahil, T., Fridman, D., Cai, K.K., Xu, S.S., Zhao, G., Zhang, M., Duan, X. X., Qin, Y., Liu, Y., 2025b. Temporal lag in nitrogen use efficiency and its implications for sustainable cropland management. Resour Conserv Recy 222.
Li, J.C., Sun, Y.X., Qin, Y., Tang, T., Kahil, T., Burek, P., Zhao, G., Cai, K.K., Jiang, Q.S., Liu, Y., 2024a. Uncovering the spatial characteristics of global net anthropogenic nitrogen input at high resolution and across 1.42 million lake basins. Sci. Total Environ. 953.
Li, J.C., Zhang, X.Y., Kahil, T., Chen, D.N., Wang, G.Y., Xu, S.S., Zhang, Y., Chen, Y., 2025c. From regional imbalances to latecomer advantage. Phosphorus Pollution and Economic Development in the Yangtze Economic Belt. Ecol Indic 173.
Li, M., Di, Z.H., Yao, Y.J., Ma, Q., 2024b. Variations in water conservation function and attributions in the Three-River Source Region of the Qinghai-Tibet Plateau based on the SWAT model. Agr Forest Meteorol 349.
Liang, L.W., Chen, M.X., Luo, X.Y., Xian, Y., 2021. Changes pattern in the population and economic gravity centers since the reform and opening up in china: the widening gaps between the south and north. J. Clean. Prod. 310.
Liu, J., Gu, W.Q., Liu, Y.W., Li, W.H., Shao, D.G., 2023. Influence of anthropogenic nitrogen inputs and legacy nitrogen change on riverine nitrogen export in areas with high agricultural activity. J. Environ. Manage. 338.
Liu, J., Zhenyao, S.Y., Yan, T.Z., Yang, Y.C., 2018. Source identification and impact of landscape pattern on riverine nitrogen pollution in a typical urbanized watershed, Beijing, China. Sci. Total Environ. 628–629, 1296–1307.
Liu, J.X., Li, Y., Zheng, Y.M., Tong, S.J., Zhang, X.C., Zhao, Y., Zheng, W., Zhai, B.N., Wang, Z.H., Zhang, X.C., Li, Z.Y., Zamanian, K., 2022. The spatial and temporal distribution of nitrogen flow in the agricultural system and green development assessment of the Yellow River Basin. Agr Water Manage 263.
Liu, L., Xu, X.L., Chen, X., 2015. Assessing the impact of urban expansion on potential crop yield in china during 1990-2010. Food Secur. 7, 33–43.
Liu, Y.X., Han, Y., Wen, X.J., Wang, C.X., Liu, T., Wang, S., 2025. All-win outcome on enhancing water-based ecosystem services with high industrial benefits in landscape restoration is spatially scarce in the yellow river basin. Ecol Front 45, 135–144.
Ma, T., Zhang, Y.Z.J., Wang, H., Tan, N.R., 2024. A multiobjective optimization model for allocating water quantity and quality in the yangtze and yellow river basins. J. Environ. Manage. 371.
Mu, J.L., Zhang, H.M., Liu, S.M., Wu, N., Song, G.D., Ding, S., Zhang, X.T., 2024. Nutrient dynamics in the Yellow River -a case study of different reservoir regulation operations. J. Hydrol. 629.
Mutascu, M., 2025. Beyond the EKC: Economic development and environmental degradation in the US. Ecol Econ 232.
Ozturk, I., Farooq, S., Majeed, M.T., Skare, M., 2024. An empirical investigation of financial development and ecological footprint in south asia: bridging the EKC and pollution haven hypotheses. Geosci. Front. 15.
Pei, W., Yan, T.Z., Lei, Q.L., Zhang, T.P., Fan, B.Q., Du, X.Z., Luo, J.F., Lindsey, S., Liu, H. B., 2022. Spatio-temporal variation of net anthropogenic nitrogen inputs (NANI). From 1991 to 2019 and Its Impacts Analysis from Parameters in Northwest China. J Environ Manage 321.
Rockstroem, J., Gupta, J., Qin, D.H., Lade, S.J., Abrams, J.F., Andersen, L.S., McKay, D.A. I., Bai, X.M., Bala, G., Bunn, S.E., Ciobanu, D., DeClerck, F., Ebi, K., Gifford, L., Gordon, C., Hasan, S., Kanie, N., Lenton, T.M., Loriani, S., Liverman, D.M., Mohamed, A., Nakicenovic, N., Obura, D., Ospina, D., Prodani, K., Rammelt, C., Sakschewski, B., Scholtens, J., Stewart-Koster, B., Tharammal, T., van Vuuren, D., Verburg, P.H., Winkelmann, R., Zimm, C., Bennett, E.M., Bringezu, S., Broadgate, W., Green, P.A., Huang, L., Jacobson, L., Ndehedehe, C., Pedde, S., Rocha, J., Scheffer, M., Schulte-Uebbing, L., de Vries, W., Xiao, C.D., Xu, C., Xu, X. W., Zafra-Calvo, N., Zhang, X., 2023. Safe and just earth system boundaries. Nature 619, 102-+.
Schaefer, S.C., Alber, M., 2007. Temporal and spatial trends in nitrogen and phosphorus inputs to the watershed of the altamaha river, Georgia, USA. Biogeochemistry 86, 231–249.
Socolow, R., 2016. Fitting on the earth: challenges of carbon and nitrogen cycle to preserve the habitability of the planet. Engineering-Prc 2, 21-+.
Sun, Y., Hao, R.F., Qiao, J.M., Xue, H., 2020. Function zoning and spatial management of small watersheds based on ecosystem disservice bundles. J. Clean. Prod. 255.
Sun, Y., Zhang, X.M., Reis, S., Chen, D.L., Xu, J.M., Gu, B.J., 2021. Dry climate aggravates riverine nitrogen pollution in australia by water volume reduction. Environ. Sci. Technol. 55, 16455–16464.
Tian, J.X., Yuan, Z., Mao, X.T., Ma, T., 2025. Quantifying natural and anthropogenic impacts on riverine total nitrogen concentration and load in the yellow river basin. Environ. Pollut. 382.
Tian, Z.G., Mu, X.Z., 2024. Towards china's dual-carbon target: energy efficiency analysis of cities in the yellow river basin based on a "geography and high-quality development" heterogeneity framework. Energy 306.
Van Meter, K.J., Basu, N.B., Van Cappellen, P., 2017. Two centuries of nitrogen dynamics: legacy sources and sinks in the mississippi and susquehanna river basins. Global Biogeochem. Cy. 31, 2–23.
Wang, C., Feng, Y.N., Xu, X.R., Zhang, X.M., Liu, H.B., Xu, J.M., Gu, B.J., 2024a. Hierarchical driving factors of ammonia emissions from cropland in China. J. Clean. Prod. 451.
Wang, G.L., Yang, D.G., Xia, F.Q., Zhong, R.S., Xiong, C.H., 2019. Three types of spatial function zoning in key ecological function areas based on ecological and economic coordinated development: a case study of tacheng basin, china. Chinese Geogr. Sci. 29, 689–699.
Wang, L.M., Xue, W.X., Si, J.J., Sheng, Z.L., 2025a. Synergizing pollution control and carbon reduction in China's Yellow River Basin: exploring the roles of policy, technology, and structural transformation. Land Use Policy 157.
Wang, W., 2025. Breaking down the barriers to clean air: the effects of china's zero-waste city policy on PM concentration. Chin J Popul Resour 23, 75–84.
Wang, Y.R., Song, J.X., Li, Q., Jiang, X.H., 2025b. Exploration of the development of water-energy-food nexus and its endogenous and exogenous drivers in the Yellow River Basin. China, J Environ Manage, p. 378.
Wang, Y.Z., Duan, X.J., Li, P.X., Wang, L.Q., 2024b. Spatiotemporal intensification of net anthropogenic nitrogen input driven by human activities in China from 1990 to 2020. Ecol Indic 160.
Wang, Z., Wang, Y.Q., Ding, X.K., Wang, Y.J., Yan, Z.Y., Wang, S.H., 2022. Evaluation of net anthropogenic nitrogen inputs in the three gorges reservoir area. Ecol. Ind. 139.
Wang, Z.S., Li, W.F., Li, Y.S., Qin, C.B., Lv, C.Y., Liu, Y., 2020. The "Three Lines One Permit" policy: An integrated environmental regulation in China. Resour Conserv Recy 163.
Wu, Z., Li, J.C., Sun, Y.X., Peñuelas, J., Huang, J.L., Sardans, J., Jiang, Q.S., Finlay, J.C., Britten, G.L., Follows, M.J., Gao, W., Qin, B.Q., Ni, J.R., Huo, S.L., Liu, Y., 2022a. Imbalance of global nutrient cycles exacerbated by the greater retention of phosphorus over nitrogen in lakes. Nat. Geosci. 15, 464–468.
Wu, Z.N., Jiang, M.M., Wang, H.L., Di, D.Y., Guo, X., 2022b. Management implications of spatial-temporal variations of net anthropogenic nitrogen inputs (NANI) in the Yellow River Basin. Environ. Sci. Pollut. R. 29, 52317–52335.
Xiao, Y.D., Liu, W.L., Zhang, F.T., Zhu, Y.L., Zhao, P., 2024. A modified approach of the agricultural grey water footprint considering the nitrogen fixation effect of crops in China. Environ. Pollut. 357.
Xie, L.M., Gao, R.Z., Wang, X.X., Duan, L.M., Fang, L.J., Tong, H., Yue, C., Liu, T.X., 2025. Spatiotemporal evolution of surface water quality and driving factors across varying levels of human interference in a major subbasin of the Yellow River Basin. China, J Hydrol-Reg Stud, p. 59.
Yang, F., Zhang, H., He, F.N., Wang, Y.F., Zhou, S.N., Dong, G.P., 2024. A 1000-year history of cropland cover change along the middle and lower reaches of the Yellow River in China. J. Geog. Sci. 34, 921–941.

Yang, M.H., Gao, X.D., Siddique, K.H.M., Wu, P.T., Zhao, X.N., 2023. Spatiotemporal exploration of ecosystem service, urbanization, and their interactive coercing relationship in the Yellow River Basin over the past 40 years. Sci. Total Environ. 858.
Yarleque, C.M.H., Shu, A.P., Liu, S.D., Tulcan, R.X.S., Zhang, Z.R., Pi, C.L., Xiao, Y.L., Zhu, F.Y., 2024. Seasonal and annual variations of sediment trapping and particulate organic carbon burial in Yellow River reservoirs. Sci. Total Environ. 954.
Ye, S.J., Wang, J.L., Jiang, J.Y., Gao, P.C., Song, C.Q., 2024. Coupling input and output intensity to explore the sustainable agriculture intensification path in mainland China. J. Clean. Prod. 442.
Yu, C.Y., Shen, W.C., Zhang, Z.F., 2025. Assessing progress toward sustainable development in China and its impact on human well-being. Environ Impact Asses 110.
Yu, G.R., Jia, Y.L., He, N.P., Zhu, J.X., Chen, Z., Wang, Q.F., Piao, S.L., Liu, X.J., He, H.L., Guo, X.B., Wen, Z., Li, P., Ding, G.A., Goulding, K., 2019. Stabilization of atmospheric nitrogen deposition in China over the past decade. Nat. Geosci. 12, 424–429.
Zhai, J.N., Han, B., Li, H.Q., Ren, W.X., Xue, B., 2023. Accounting for the nitrogen footprint of food production in chinese provinces during 1998-2018. J. Clean. Prod. 389.
Zhang, C.Y., Oki, T., 2024. Water transfer contributes to water resources management: Crisis mitigation for future water allocation in the Yellow River basin. Iscience 27.
Zhang, S., Zhang, L.L., Meng, Q.Y., Wang, C.C., Ma, J.J., Li, H., Ma, K., 2024a. Evaluating agricultural non-point source pollution with high-resolution remote sensing technology and SWAT model: a case study in Ningxia Yellow River Irrigation District. China, Ecol Indic, p. 166.
Zhang, S.H., Li, X., Ren, Z., Zhang, C., Fang, L., Mo, X.B., Yang, W., Liu, X.H., 2025a. Influence of precipitation and temperature variability on anthropogenic nutrient inputs in a river watershed: Implications for environmental management. J. Environ. Manage. 375.
Zhang, X.N., Ward, B.B., Sigman, D.M., 2020. Global Nitrogen Cycle: critical Enzymes, Organisms, and Processes for Nitrogen Budgets and Dynamics. Chem. Rev. 120, 5308–5351.
Zhang, Z., Wang, Q., Yan, F.Q., Sun, Y.J., Yan, S.J., 2024b. Revealing spatio-temporal differentiations of ecological supply-demand mismatch among cities using ecological Network: A case study of typical cities in the "Upstream-Midstream-Downstream" of the Yellow River Basin. Ecol Indic 166.
Zhang, Z.H., Yan, D., Li, M.M., Lu, Y.T., Zhou, Y.T., Wang, T.J., Zhuang, B.L., Li, S., Huang, X., 2025b. Drivers for the trends of atmospheric inorganic nitrogen deposition in china under the past and future scenarios. Atmos. Environ. 352.
Zhao, J.H., Chen, W., Liu, Z.X., Liu, W., Li, K.Y., Zhang, B., Zhang, Y.G., Yu, L., Sakai, T., 2024. Urban expansion, economic development, and carbon emissions: Trends, patterns, and decoupling in mainland China's provincial capitals (1985-2020). Ecol Indic 169.
Zhao, M.M., Wang, S.M., Chen, Y.P., Wu, J.H., Xue, L.G., Fan, T.T., 2020. Pollution status of the Yellow River tributaries in middle and lower reaches. Sci. Total Environ. 722.
Zhao, Z.Y., Zhang, L.X., Deng, C.N., 2022. Changes in net anthropogenic nitrogen and phosphorus inputs in the Yangtze River Economic Belt, China (1999-2018). Ecol Indic 145.
Zheng, C.J., Deng, F., Li, C.Y., Yang, Z.M., 2022. The impact of China's western development strategy on energy conservation and emission reduction. Environ Impact Asses 94.
Zheng, J.Q., Cao, X.H., Ma, C.Z., Weng, N.Y., Huo, S.L., 2023. What drives the change of nitrogen and phosphorus loads in the Yellow River Basin during 2006-2017? J. Environ. Sci. 126, 17–28.
Zhong, W.J., Wang, S.R., Dong, Y., Ni, Z.K., Fan, Y., Wu, D.S., 2022. Trends of the response-relationship between net anthropogenic nitrogen and phosphorus inputs (NANI/NAPI) and TN/TP export fluxes in Raohe basin. China, Chemosphere, p. 286.
Zhou, J.H., Liu, X.H., Liu, X.J., Wang, W.L., Wang, L.Q., 2023. Assessing agricultural non-point source pollution loads in typical basins of upper Yellow River by incorporating critical impacting factors. Process Saf Environ 177, 17–28.